PHYSICAL REVIEW E **93**, 060203(R) (2016)

Barrier-induced chaos in a kicked rotor: Classical subdiffusion and quantum localization

Sanku Paul,[1,*] Harinder Pal,[2,†] and M. S. Santhanam[1,‡]

[1]*Indian Institute of Science Education and Research, Dr. Homi Bhabha Road, Pune 411 008, India*

[2]*Instituto de Ciencias Físicas, Universidad Nacional Autónoma de México, Codigo Postal 62210, Cuernavaca, Mexico*

(Received 30 March 2016; published 30 June 2016)

The relation between classically chaotic dynamics and quantum localization is studied in a system that violates the assumptions of the Kolmogorov-Arnold-Moser (KAM) theorem, namely, the kicked rotor in a discontinuous potential barrier. We show that the discontinuous barrier induces chaos and more than two distinct subdiffusive energy growth regimes, the latter being an unusual feature for Hamiltonian chaos. We show that the dynamical localization in the quantized version of this system carries the imprint of non-KAM classical dynamics through the dependence of quantum break time on subdiffusion exponents. We briefly comment on the experimental feasibility of this system.

DOI: 10.1103/PhysRevE.93.060203

The interplay between disorder, in the form of chaotic classical dynamics, and quantum localization continues to attract attention due to a rich variety of its manifestations. The kicked rotor (KR), in which a particle is periodically kicked by an external field, is a paradigmatic example for both chaos and localization [1]. From a dynamics point of view, the classical KR, for large kick strengths, displays chaos and energy diffusion [2]. The suppression of diffusion in the quantum regime results from destructive quantum interference and is termed dynamical localization (DL) due to its analogy with Anderson localization [2,3]. Dynamical localization was experimentally observed in an atom-optics-based realization of the KR [4]. The emergence of quantum localization in the variants of a KR has led to novel scenarios for quantum ratchets [5], classical-quantum correspondence [6], coherent quantum control [7], metal-insulator transition [8], nonlinearity effects [9], and decoherence [10]. Recently, an unusual classical "dynamical localization" was reported as well [11].

A kicked rotor is a system that obeys the Kolmogorov-Arnold-Moser (KAM) theorem [2] implying that the transition from regular to predominantly chaotic dynamics happens gradually by breakup of invariant tori upon variation of a control parameter. We have obtained a good understanding of diffusion and localization effects in the KR as a representative KAM system [2]. Comparatively, much less is known about chaotic systems that violates the assumptions of the KAM theorem, the so-called non-KAM systems. Theoretical studies of non-KAM systems such as the kicked oscillator [12], kicked particle in potential well configurations [13,14] have revealed an abrupt transition from integrability to chaos leading to global transport due to the absence of invariant tori that fragments phase space. In fact, experiments on non-KAM systems have exploited this property to enhance or, in general, control electronic transport in semiconductor superlattices [15] and in coupled billiards in the form of two-dimensional electron gas in an external magnetic field [16].

In spite of global classical transport, quantum localization can suppress transport. In chaotic systems, localization takes various forms. In time-dependent systems such as KR, DL is a purely quantum effect that disregards classical dynamics beyond certain time scales called break time. In autonomous chaotic systems like the atoms in strong magnetic fields and coupled oscillators [17] semiclassical scarring localization arises due to the influence of isolated unstable periodic orbits [18]. Partial barriers in classical phase space, cantori [19], can also lead to localization as in the case of ionic motion in a Paul trap [20] and in a special case of Bunimovich billiards modeled as a discontinuous quantum map [21]. The classical analog of the latter system violates the KAM theorem.

Generally, quantum-classical correspondence in non-KAM systems has not been studied in detail and promises new insights in view of the rich classical dynamical features. Motivated by this, we report on a non-KAM classical feature, subdiffusive transport induced by discontinuous potential barriers rather than by cantori, and its relation to quantum localization. We note that in Hamiltonian systems anomalous transport arising due to the presence of sticky islands in chaotic sea is generally superdiffusive in nature and subdiffusive behavior is not seen [22].

Currently, quantum localization in disordered media with correlated disorder is vigorously investigated, both in theory and experiments [23]. Thus, our results are also relevant in the broader context of the continuing interest in anomalous diffusion [24] and localization properties of wave phenomena in different areas [25].

The dimensionless Hamiltonian for a kicked rotor in potential barriers is

$$H = \frac{p^2}{2} + V(q) + \varepsilon \cos(q) \sum_{n=-\infty}^{\infty} \delta(t-n), \qquad (1)$$

where $H_0 = \frac{p^2}{2} + V(q)$ is the unperturbed system with

$$V(q) = V_0[\theta(q - R\pi - \phi) - \theta(q - R\pi - b - \phi)] \qquad (2)$$

being the stationary potential depicted in Fig. 1(a), $\theta(\cdot)$ is the unit step function, V_0 and b are the height and width of the potential barrier, respectively, ε is the kick strength, ϕ is the phase of the kicking field, and $R = w/\lambda$ is the ratio of width of the well to the wavelength of the kicking field.

*sankup005@gmail.com
†harinder101@gmail.com
‡santh@iiserpune.ac.in

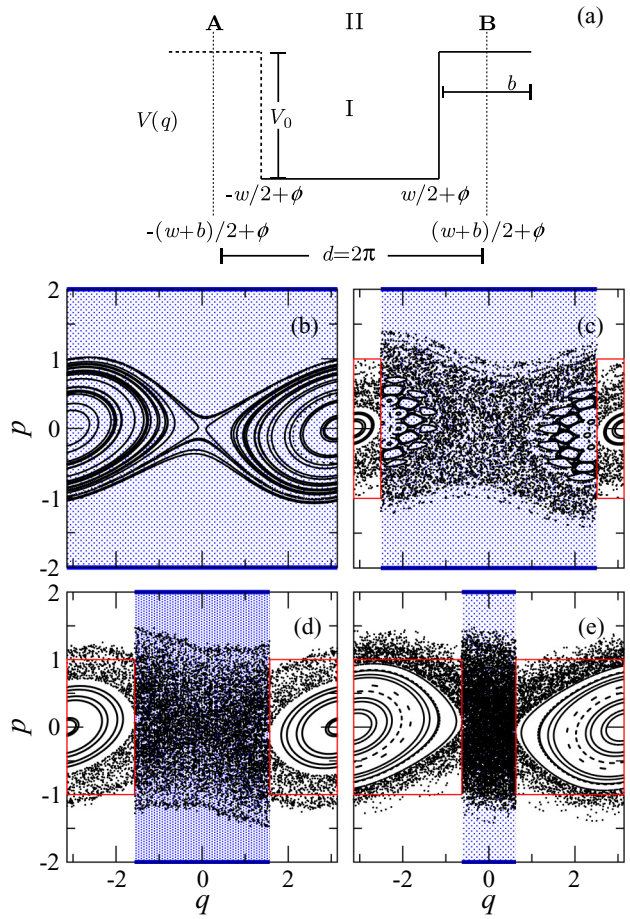

FIG. 1. (a) Schematic of the stationary potential $V(q)$ with $\phi = 0$ and $\lambda = 2\pi$. Periodic boundary conditions imposed at positions A and B. The regions below and above V_0 are denoted by I and II. (b)–(e) display the stroboscopic sections. The barrier regions are marked as (red) rectangular boxes and the well region is hatched (blue). The parameters are $V_0 = 0.5$, $\phi = 0.0$, and $\varepsilon = 0.25$. The width of the well region w is (b) 2π, (c) 1.6π, (d) π, and (e) 0.4π.

Physically, Eq. (1) represents a kicked particle in a potential $V(q)$ with periodic boundary conditions applied at positions $q = \pm(w + b)/2$. Throughout this Rapid Communication, we choose $\phi = 0$, $w + b = 2\pi$, $\lambda = 2\pi$ and consequently, $0 < R < 1$. For convenience, we denote the regions below and above the barrier height V_0 as I and II. In general, the dynamics of the system is determined by V_0, ε, and either R or b. The classical dynamics can be explicitly reduced to a map on a suitably chosen stroboscopic section [26].

If $V_0 = 0$, then Eq. (1) reduces to a kicked rotor on an infinite cylinder. For $\varepsilon = 0$, it is a classically integrable system. If $V_0 > 0$, the potential $V(q)$ is nonanalytic and violates the assumptions of the KAM theorem. Thus, when external kicks are introduced with $\varepsilon > 0$, KAM tori that partition the phase space are destroyed, even if ε is arbitrarily small, leading to chaotic dynamics. Figures 1(b)–1(e) show stroboscopic sections obtained by evolving the classical map for kick strength $\varepsilon = 0.25$ with several values of w. The nature of dynamics can be understood in terms of that of the kicked rotor [$V_0 = 0$ in Eq. (1)]. We recall that for identical value of kick strength, and indeed for any value of $\varepsilon \ll 1$, the phase space of the kicked rotor is covered with invariant tori $I_{\mathrm{KR}}(\omega)$ characterized by winding number ω. In the presence of barriers, a particle initially on a kicked rotor tori $I_{\mathrm{KR}}(\omega)$ would continue to evolve on it until interrupted by the barrier discontinuities at $q = -w/2$ or $w/2$. This results in reflection ($q \to q, p \to -p$) or refraction ($q \to q, p \to \pm\sqrt{p^2 - 2V_0}$) of the particle and it hops onto another tori $I'_{\mathrm{KR}}(\omega')$, with $\omega \neq \omega'$. Every barrier encounter leads to tori hopping. As $n \gg 1$, multiple barrier encounters and the resulting tori hopping ensure that the autocorrelations decay quickly, resulting in chaotic dynamics [Figs. 1(c)–1(e)] and diffusion of the energy absorbed from periodic kicks. This is one manifestation of non-KAM type dynamics in which barriers play a crucial role in the genesis of chaos and energy diffusion.

However, if the condition $\pm R\pi + \phi = \pi l, l \in \mathbb{Z}$ is satisfied in region I, then $I_{\mathrm{KR}}(\omega)$ are preserved even with the barrier encounters [14]. This leads to KAM-like tori in region I as shown for $b = 0.0$ in Fig. 1(b). It can be shown that the dynamics is completely hyperbolic if $R < 0.5$ and $\phi = 0$ [13]. A physically interesting scenario for energy transport arises if $l \notin \mathbb{Z}$ leading to non-KAM chaos in region I, and region II displays invariant tori but punctured by the discontinuities in the potential. In the rest of the Rapid Communication, we choose parameters (listed in Fig. 2) satisfying these conditions. This choice ensures an absence of complete dynamical barriers and cantori are not effective as barriers to transport. Under these conditions, as kicks impart energy, global subdiffusive transport becomes possible since the chaotic

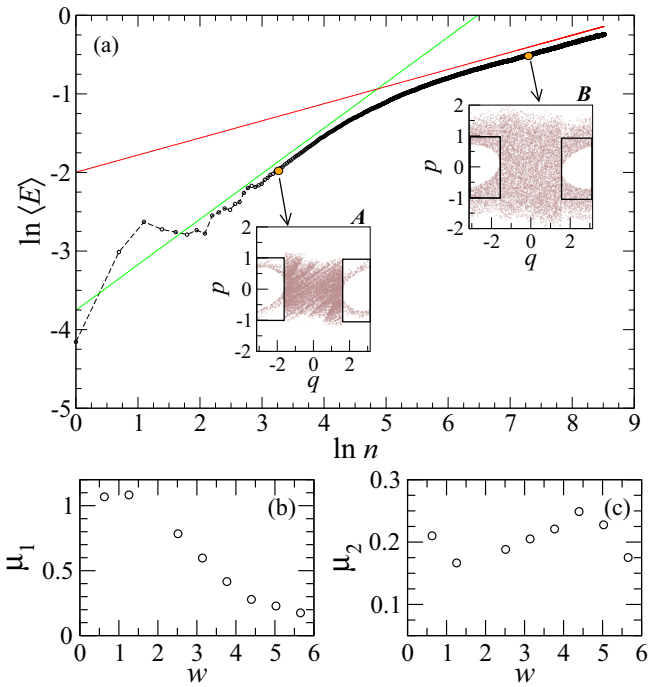

FIG. 2. The growth of mean energy $\langle E \rangle$ vs n for parameters $V_0 = 0.5$, $w = \pi$, and $\varepsilon = 0.25$. The two solid lines (green and red) fit the linear regimes in the log-log plot. The insets display the stroboscopic sections at the 25th kick (A) and at the 1500th kick (B). (b), (c) The dependence of μ_1 and μ_2 on w.

particles in region I penetrate through the punctured tori into region II.

The classical mean energy growth is subdiffusive and displays two distinct power-law regimes within experimentally accessible time scales. Figure 2(a) illustrates classical mean energy $\langle E\rangle$ as a function of time (in units of kick period) for the same set of parameters as in Fig. 1(d). The initial condition is an ensemble of points with $-w/2 < q < w/2$ and $p = 0$. The first subdiffusive regime in Fig. 2(a) and the accompanying stroboscopic section (inset A) show that most of the particles are physically confined to the well in region I. Note that the mean energy growth can be described by $\langle E\rangle_n \sim D_1 n^{\mu_1}$, where D_1 is the diffusion coefficient and $0 < \mu_1 \leqslant 1$ is the exponent. This subdiffusive behavior can be attributed to correlations. In general, the phase space in region I can be mixed [intricate chain of islands in a chaotic sea as in Fig. 1(c)] for $R > 0.5$ or completely chaotic for $R < 0.5$ if $V_0 \gg 1$. When $R > 0.5$, the energy growth is suppressed significantly due to the correlations induced by a combination of factors: (i) dynamics on $I_{\rm KR}(\omega)$ between successive tori hops, (ii) stickiness in the vicinity of the chain of islands, and (iii) slow diffusion through the punctured tori in region II. When $R < 0.5$, even though the phase space appears chaotic due to tori hops, correlations of type $\langle q_n q_{n+N}\rangle \propto N^{-\gamma}$ exist because the evolution between two successive barrier encounters is confined to a kicked rotor tori $I_{\rm KR}(\omega)$. By tuning the number of barrier encounters in one kick period we can enhance or suppress correlations. As $w \to 0$, the barrier encounters and tori hops in one kick period increase and hence $\mu_1 \to 1$ [see Figs. 2(b) and 3(a)], the quasilinear diffusion limit [1,2] expected under conditions of predominant chaos.

We formally define $\tau_1 = (D_1/D_2)^{1/(\mu_2-\mu_1)}$ as the time at which the first subdiffusive regime characterized by $\{D_1,\mu_1\}$ crosses over to the second characterized by $\{D_2,\mu_2\}$. The second regime begins after the particles enter region II for $n > \tau_1$, as seen in inset B in Fig. 2. The energy growth is subdiffusive with $\langle E\rangle_n \sim D_2 n^{\mu_2}$, $0 < \mu_2 < 1$. In region II, we expect the phase space to display kicked rotor tori $I_{\rm KR}(\omega)$ punctured by the discontinuities in $V(q)$. Note that one complete crossing of a barrier of width $b > 0$ involves two refractions, at say, $q = w/2$ and $q = (w/2) + b$. When a particle with energy E_0 enters the above-barrier region and assuming that it does not suffer any kick while transiting this region, the net change in position between the last and the next kick is denoted by Δq. If $\Delta q_{\rm KR}$ represents a similar quantity for the kicked rotor ($V_0 = 0$), we can show that $\delta q = |\Delta q - \Delta q_{\rm KR}| = b(\beta - 1)$, where $\beta = (1 - V_0/E_0)^{-1/2}$. Clearly, if $E_0 \gtrsim V_0$, then $\delta q \gg 0$ and if $E_0 \gg V_0$ we have $\delta q \to 0$. This difference leads to torus hopping. Further, as $\delta q \neq 0$, it translates into momentum difference $\delta p = |\Delta p - \Delta p_{KR}| = \varepsilon|\sin[q_k - (p/|p|)\delta q] - \sin q_k|$ at the position of the next kick q_k. Thus, if $E_0 \gtrsim V_0$, the invariant tori do not survive due to large tori hopping induced by the discontinuities. This appears as chaotic dynamics in region II in inset B of Fig. 2. On the other hand, if $E_0 \gg V_0$, then invariant tori are largely preserved with minor dispersion and hence the tori hopping is a negligible effect. A similar result can be obtained even if the particle suffers kicks while transiting the barrier region. For $n > \tau_1$, ignoring a short transient, multiple barrier-induced refractions interspersed with dynamics on $I_{\rm KR}(\omega)$ leads to classical energy growth that is slower than normal diffusive growth. This regime lasts until a time scale of $\tau_2 \approx 10^4\tau_1$ (in units of kick period) by which time the particles evolve to the vicinity of resonance structure at $|p| = 2\pi$. This can be thought of as long-lasting since τ_2 is much longer than the experimentally relevant time scale with atom optics as the test bed. This subdiffusion mechanism has a weak though systematic dependence on w. As Figs. 2(c) and 3(b) reveal, $\mu_2 \approx 0.2$ to a first approximation.

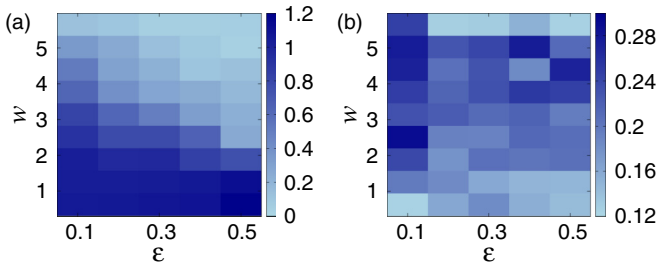

FIG. 3. Subdiffusion exponents μ_1 (a) and μ_2 (b) plotted as a function of w and ε. Subdiffusion occurs over a wide range of parameter values.

To the best of our knowledge, long-lasting subdiffusion in chaotic Hamiltonian systems has not been reported before, though it was observed in the quantum dynamics of nonlinear disordered systems [27] and phase randomized, double kicked rotor [28]. Generally, anomalous diffusion in chaotic Hamiltonians is of the superdiffusive type due to stickiness or the presence of accelerator modes in phase space [19,22,29]. Further, for bounded and ergodic systems, superdiffusion follows as a consequence of Kac's theorem [19,30] which guarantees that the mean recurrence time exists. However, the phase space of the system in Eq. (1) being an infinite cylinder, is not bounded and Kac's theorem does not strictly apply. The subdiffusion induced by the potential barriers combined with unbounded phase space is associated with diverging mean recurrence times (not shown here).

Next, we focus on the quantum regime of the Hamiltonian in Eq. (1). The period-1 Floquet operator for this kicked system can be obtained as

$$\widehat{U} = \exp\left(-\frac{i\varepsilon}{\hbar_s}\cos\widehat{q}\right)\exp\left(-\frac{i}{\hbar_s}\left[\frac{\widehat{p}^2}{2} + \widehat{V}\right]\right), \quad (3)$$

where $\hbar_s = \frac{2\pi^2\hbar}{E_c T}$ is the scaled Planck's constant and $E_c = \frac{m\lambda^2}{2T^2}$ (T is the kicking period). In this, $\psi(q,n) = \hat{U}^n\psi(q,0)$ for any arbitrary initial wave packet $\psi(q,0)$. The classical limit will correspond to taking $\hbar_s \to 0$ keeping ε constant. First, we solve the Schrödinger equation for the unperturbed system, $H_0 u_m = \lambda_m u_m$, using momentum eigenstates as the basis, i.e., $u_m(q) = (\frac{1}{\sqrt{2\pi}})\sum_p a_{m,p}e^{-ipq}$, $p = 0,\pm1,\pm2,\ldots$, where $a_{m,p}$ are the expansion coefficients. The Floquet operator written in the basis of u_m is

$$U_{mn} = e^{-i\lambda_n/\hbar_s}\sum_{p,p'} a^*_{m,p}a_{n,p'}(-i)^{|p-p'|}J_{|p-p'|}\left(\frac{\varepsilon}{\hbar_s}\right) \quad (4)$$

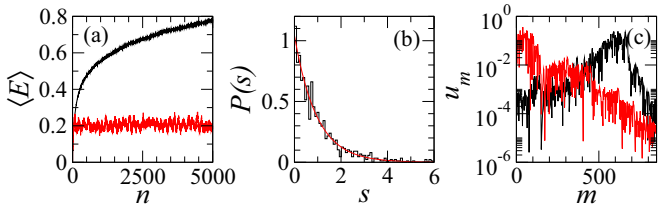

FIG. 4. (a) The classical (black) and quantum (red) mean energy growth with parameters $V_0 = 0.5$, $\phi = 0.0$, $w = \pi$, $\varepsilon = 0.25$, and $\hbar_s = 0.0067$. (b) The nearest neighbor spacing distribution of Floquet phases (histogram) and Poisson distribution (solid line). (c) Two Floquet states in the unperturbed basis (in semilogarithmic scale).

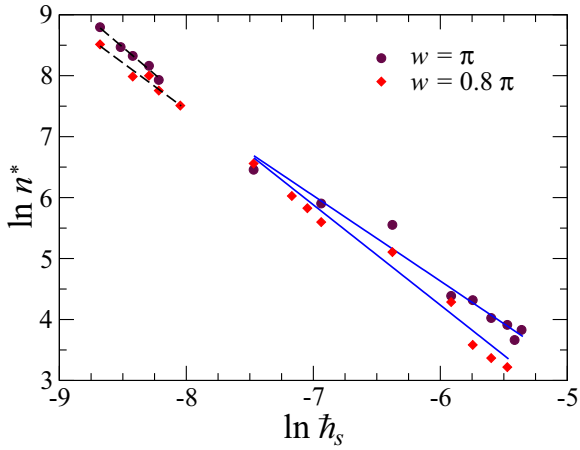

FIG. 5. Scaling of quantum break time with the scaled Planck's constant $\hbar_s$ for two well widths w. The parameters are $V_0 = 0.5$, $\phi = 0.0$, and $\varepsilon = 0.25$. The solid lines and dashed lines have slope $-2/(2-\mu)$ [see Eq. (5)], with $\mu = \mu_1$ and $\mu = \mu_2$, respectively (see text for details).

in which $J_l(\cdot)$ is the Bessel function of order l. By numerically solving the eigenvalue equation $\widehat{U}\xi_i = e^{i\phi_i}\xi_i$, we obtain the Floquet phases ϕ_i and Floquet states ξ_i for $i = 1,2,3,\ldots,N$, where N is the number of basis states (eigenstates of H_0).

We evolve an initial wave packet $\psi(q,0)$, chosen to be the ground state of H_0, under the action of $\widehat{U}$ and its quantum mean energy $\langle E\rangle$ is displayed in Fig. 4(a). Clearly, the quantum $\langle E\rangle$ does not follow the subdiffusive behavior of the classical dynamics beyond a certain time scale and instead saturates indicating a localization effect in energy basis. From the point of view of random matrix theory, this system falls in the class of circular orthogonal ensemble (COE). Although we expect Wigner distribution for the spacings of Floquet phases, quantum localization of the Floquet states leads to uncorrelated spacings and Poisson distribution. This is shown in Fig. 4(b) and is similar to that of the kicked rotor with connections to Anderson localization [3]. The Floquet states in the unperturbed basis, shown in Fig. 4(c), display exponential localization. As $\hbar_s \to 0$, all the Floquet states are localized although the localization lengths diverge as $\hbar_s^{-2/(2-\mu)}$, μ being one of the subdiffusion exponents, and the spectral statistics transits from Poisson to COE distribution.

We discuss how the non-KAM nature of the Hamiltonian in Eq. (1) manifests in the quantum domain. As shown before, the classical subdiffusion of energy arises due to hopping between KR tori $I_{\rm KR}(\omega)$ or punctured tori, a feature facilitated by the discontinuous potential barriers. The time scale over which the quantum dynamics follows classical is related to the inverse of mean spacing of the Floquet spectrum. Assuming that the mean level density $\rho(E)$ of the unperturbed system near the ground state is proportional to $E^{-1/2}$, we obtain an estimate for quantum break time n^* to be

$$n^* \sim \sqrt{\alpha}\left(\frac{D_i}{2\pi^2\hbar_s^2}\right)^{1/(2-\mu_i)}, \qquad (5)$$

where $i = 1$ or 2 corresponding to any one of the two classical subdiffusive regimes and α is a constant. Significantly, the non-KAM nature of the system leaves its imprint in the quantum domain through the dependence of n^* on diffusion exponents μ_1 or μ_2. For relatively large values of $\hbar_s$, $n^* < \tau_1$ and the scaling exponent is $-2/(2-\mu_1)$ depending on the first classical subdiffusive regime with exponent μ_1. As $\hbar_s \to 0$, we have $n^* > \tau_1$ and the scaling exponent is $-2/(2-\mu_2)$, corresponding to the second classical subdiffusive regime with exponent μ_2. As shown in Fig. 5, a log-log plot of n^* against $\hbar_s$ shows linear behavior and agrees well with the theoretically expected slope $-2/(2-\mu)$, $\mu = \mu_1$ or μ_2. This is shown for two sets of parameters. Thus, by varying either w or λ, the classical diffusion rate can be controlled leading to a tunable quantum break time n^*. As $\hbar_s \to 0$, the quantum energy diffusion rate and the length of diffusive time scale n^* can both be controlled by manipulating system parameters.

In the limit of $\varepsilon \gg 1$, the system displays predominantly chaotic dynamics. The potential barriers play only a marginal role in the genesis of chaos and we obtain a single normal diffusion regime similar to the case of the kicked rotor. As would be expected, the quantum dynamics displays dynamical localization. The central results discussed here, barrier-induced chaos and subdiffusive dynamics and its quantum manifestations, would be valid for a larger class of kicked particles placed in barrier-type potentials of various configurations. We comment on the experimental feasibility of this system. The kicked rotor was realized using cold atoms in optical lattices created by two counterpropagating pulsed laser beams [4]. To experimentally realize a kicked particle in potential barriers, an additional set of laser beams, that are always on, can be used to create a confining potential with large barrier height. A periodically kicked particle in a single confining potential barrier was experimentally realized nearly a decade back [31]. While this setup could be extended, it is also possible to achieve this using semiconductor heterostructures [15].

In summary, we study the classical and quantum dynamics of a kicked particle interacting with a discontinuous potential. In this non-KAM system, chaos and subdiffusion are induced by the encounters of the particle with the discontinuous barriers. The classical mean energy displays more than two distinct regimes of *subdiffusive* growth. In the quantum domain, the Floquet states are localized in the energy basis. Significantly, the non-KAM nature of the system manifests

in the quantum regime through the dependence of quantum break time on subdiffusion exponents, leading to a tunable break time. These results can be generalized for various discontinuous potential configurations.

H.P. acknowledges UNAM/DGAPA/PAPIIT research Grant No. IG100616 and support through a post-doctoral fellowship from DGAPA-UNAM. S.P. would like to thank CSIR-UGC for support through the research fellowship.

[1] F. M. Izrailev, Phys. Rep. **196**, 299 (1990).
[2] L. Reichl, *The Transition to Chaos: Conservative Classical Systems and Quantum Manifestations* (Springer, New York, 2004).
[3] D. R. Grempel, R. E. Prange, and S. Fishman, Phys. Rev. A **29**, 1639 (1984).
[4] F. L. Moore, J. C. Robinson, C. F. Bharucha, B. Sundaram, and M. G. Raizen, Phys. Rev. Lett. **75**, 4598 (1995).
[5] T. S. Monteiro, P. A. Dando, N. A. C. Hutchings, and M. R. Isherwood, Phys. Rev. Lett. **89**, 194102 (2002).
[6] B. Gadway, J. Reeves, L. Krinner, and D. Schneble, Phys. Rev. Lett. **110**, 190401 (2013); J. Wang and A. M. Garcia-Garcia, Int. J. Mod. Phys. B **22**, 5261 (2008).
[7] J. Gong and P. Brumer, Phys. Rev. Lett. **86**, 1741 (2001); J. Gong, H. J. Worner, and P. Brumer, Phys. Rev. E **68**, 056202 (2003).
[8] I. Manai, J. F. Clement, R. Chicireanu, C. Hainaut, J. C. Garreau, P. Szriftgiser, and D. Delande, Phys. Rev. Lett. **115**, 240603 (2015); A. M. Garcia-Garcia and J. Wang, *ibid.* **94**, 244102 (2005); P. Qin, C. Yin, and S. Chen, Phys. Rev. B **90**, 054303 (2014); R. Dutta and P. Shukla, Phys. Rev. E **78**, 031115 (2008); J. Wang and A. M. Garcia-Garcia, *ibid.* **79**, 036206 (2009).
[9] L. Ermann and D. L. Shepelyansky, J. Phys. A **47**, 335101 (2014); M. V. Ivanchenko, T. V. Laptyeva, and S. Flach, Phys. Rev. B **89**, 060301(R) (2014); D. S. Brambila and A. Fratalocchi, Sci. Rep. **3**, 2359 (2013); G. Gligoric, J. D. Bodyfelt, and S. Flach, Europhys. Lett. **96**, 30004 (2011).
[10] H. Schomerus and E. Lutz, Phys. Rev. Lett. **98**, 260401 (2007).
[11] I. Guarneri, G. Casati, and V. Karle, Phys. Rev. Lett. **113**, 174101 (2014).
[12] S. A. Gardiner, J. I. Cirac, and P. Zoller, Phys. Rev. Lett. **79**, 4790 (1997).
[13] R. Sankaranarayanan, A. Lakshminarayan, and V. B. Sheorey, Phys. Rev. E **64**, 046210 (2001); Phys. Lett. A **279**, 313 (2001); B. Hu, B. Li, J. Liu, and Y. Gu, Phys. Rev. Lett. **82**, 4224 (1999).
[14] Harinder Pal and M. S. Santhanam, Phys. Rev. E **82**, 056212 (2010); Pramana **77**, 793 (2011).
[15] T. M. Fromhold *et al.*, Nature (London) **428**, 726 (2004); T. M. Fromhold, A. A. Krokhin, C. R. Tench, S. Bujkiewicz, P. B. Wilkinson, F. W. Sheard, and L. Eaves, Phys. Rev. Lett. **87**, 046803 (2001).
[16] R. Brunner, R. Meisels, F. Kuchar, R. Akis, D. K. Ferry, and J. P. Bird, Phys. Rev. Lett. **98**, 204101 (2007); R. Brunner *et al.*, Physica E **40**, 1315 (2008).
[17] K. Muller and D. Wintgen, J. Phys. B **27**, 2693 (1998); H. Friedrich and D. Wintgen, Phys. Rep. **183**, 37 (1989); M. S. Santhanam, V. B. Sheorey, and A. Lakshminarayan, Phys. Rev. E **57**, 345 (1998).
[18] E. J. Heller, Phys. Rev. Lett. **53**, 1515 (1984).
[19] J. D. Meiss, Chaos **25**, 097602 (2015); R. S. MacKay, J. D. Meiss, and I. C. Percival, Phys. Rev. Lett. **52**, 697 (1984).
[20] M. ElGhafar, P. Torma, V. Savichev, E. Mayr, A. Zeiler, and W. P. Schleich, Phys. Rev. Lett. **78**, 4181 (1997); S. W. Kim and H-W. Lee, Phys. Rev. E **61**, 5124 (2000).
[21] F. Borgonovi, Phys. Rev. Lett. **80**, 4653 (1998); F. Borgonovi *et al.*, Physica D **131**, 317 (1999).
[22] E. G. Altmann and H. Kantz, in *Anomalous Transport: Foundations and Applications*, edited by R. Klages, G. Radons, and I. M. Sokolov (Wiley-VCH, Weinheim, 2008).
[23] F. Jendrzejewski *et al.*, Nat. Phys. **8**, 398 (2012); F. M. Izrailev, A. A. Krokhin, and N. M. Makarov, Phys. Rep. **512**, 125 (2012).
[24] *Anomalous Transport: Foundations and Applications*, edited by R. Klages, G. Radons, and I. M. Sokolov (Wiley-VCH, Weinheim, 2008).
[25] C. Liu *et al.*, Nat. Phys. **11**, 358 (2015); M. Segev, Y. Silberberg, and D. N. Christodoulides, Nat. Photon. **7**, 197 (2013); Y. Lahini, A. Avidan, F. Pozzi, M. Sorel, R. Morandotti, D. N. Christodoulides, and Y. Silberberg, Phys. Rev. Lett. **100**, 013906 (2008); J. Floss, S. Fishman, and I. S. Averbukh, Phys. Rev. A **88**, 023426 (2013).
[26] See Supplemental Material at http://link.aps.org/supplemental/10.1103/PhysRevE.93.060203 for the classical map.
[27] A. S. Pikovsky and D. L. Shepelyansky, Phys. Rev. Lett. **100**, 094101 (2008); S. Flach, D. O. Krimer, and Ch. Skokos, *ibid.* **102**, 024101 (2009); T. Schwartz, G. Bartal, S. Fishman, and M. Segev, Nature (London) **446**, 52 (2007); M. Mulansky, K. Ahnert, and A. Pikovsky, Phys. Rev. E **83**, 026205 (2011); M. Mulansky and A. Pivkovsky, New J. Phys. **15**, 053015 (2013).
[28] J. Wang, T. S. Monteiro, S. Fishman, J. P. Keating, and R. Schubert, Phys. Rev. Lett. **99**, 234101 (2007).
[29] T. Manos and M. Robnik, Phys. Rev. E **89**, 022905 (2014).
[30] M. Kac, Bull. Am. Math. Soc. **53**, 1002 (1947).
[31] K. Henderson *et al.*, Europhys. Lett. **75**, 392 (2006).